

# Diachronic mapping and evaluation of soil erosion rates using RUSLE in the Bouregreg River Watershed, Morocco

Fouad Moudden<sup>1)</sup>✉, Mohammed El Hafyani<sup>1)</sup>, Anas El Ouali<sup>2)</sup>, Allal Roubil<sup>1)</sup>,  
Abdelhadi El Ouali<sup>1)</sup>, Ali Essahlaoui<sup>1)</sup>, Youssef Brouziyne<sup>3)</sup>

<sup>1)</sup> Moulay Ismail University, Faculty of Sciences, Department of Geology, Laboratory of Geoengineering and Environment, Research Group "Water Sciences and Environment Engineering, Zitoune, Meknes BP11201, Morocco

<sup>2)</sup> Sidi Mohamed Ben Abdellah University, Faculty of Science and Technology, Functional Ecology and Environmental Engineering Laboratory, Fez, Morocco

<sup>3)</sup> Mohammed VI Polytechnic University, International Water Research Institute, Ben Guerir, Morocco

RECEIVED 15.02.2021

ACCEPTED 23.08.2021

AVAILABLE ONLINE 20.06.2022

**Abstract:** Soil erosion has been severely affecting soil and water resources in semi-arid areas like the Mediterranean. In Morocco, this natural process is accelerated by anthropogenic activities, such as unsustainable soil management, overgrazing, and deforestation. With a drainage area of 395,600 ha, the Bouregreg River Watershed extends from the Middle Atlas Range (Jebel Mtourzgane) to the Sidi Mohamed Ben Abdellah (SMBA) dam reservoir south-east of Rabat. Its contrasted eco-geomorphological landscapes make it susceptible to unprecedented soil erosion due to climate change. Resulting changes in erosive dynamics led to huge amounts of solid loads transported to the catchment outlet and, thus, jeopardised the SMBA dam lifespan due to siltation.

The research aims to quantify the average annual soil losses in this watershed using the Revised Universal Equation of Soil Losses (RUSLE) within a GIS environment. To highlight shifts in land use/land cover patterns and their effects on erosional severity, we have resorted to remote sensing through two Landsat 8 satellite images captured in 2004 and 2019. The C factor was combined with readily available local data regarding major erosion factors, e.g. rainfall aggressiveness (*R*), soil erodibility (*K*), topography (*LS*), and conservation practices (*P*). The helped to map the erosion hazard and determine erosion prone areas within the watershed where appropriate water and conservation measures are to be considered. Accordingly, from 2004 to 2019, average annual soil losses increased from 11.78 to 18.38 t·ha<sup>-1</sup>·y<sup>-1</sup>, as the watershed area affected by strong erosion (>30 t·ha<sup>-1</sup>·y<sup>-1</sup>) evolved from 13.57 to 39.39%.

**Keywords:** Bouregreg Watershed, diachronic mapping GIS, Revised Universal Equation of Soil Losses (RUSLE) model, water erosion

## INTRODUCTION

"If the land and soils are degraded, the humankind will suffer the same fate" [LAL 2019]. Human pressure on soil resources is beyond tolerable threshold and threaten the safeguarding of ecosystem services and biodiversity [FAO 2014]. Consequently, the Global Soil Partnership (GSP) endeavours to promote soil security [FAO 2014] through establishing the Voluntary Guidelines for Sustainable Soil Management (VGSSM).

Soil erosion is recognised to be the worst driver of land degradation. Its water driven form is the most threatening to world's soil resources. It leads to a huge global soil loss of nearly (20–30)·10<sup>9</sup> t as compared to that of tillage erosion 5·10<sup>9</sup> t per year and generates fluxes ranging from 23·10<sup>6</sup> to 42·10<sup>6</sup> t of nitrate and 14.6·10<sup>6</sup> to 26.4·10<sup>6</sup> t of phosphorus per year [FAO 2014]. Water soil erosion on-site damaging impacts are: land and cropping fields' health degradation, soil productivity reduction, and the undermining of ecosystem services and biodiversity.

Several studies point to downstream water bodies' eutrophication, water quality reduction by transported sediments, nutrients, chemicals and fertilisers, dam siltation, water bodies destruction (mainly water reservoirs), and the reduction of fish stocks in hydrosystems as severe off-site impacts of this erosion form.

Recently, there are evidence-based indicators of significant shifts in land use [BORRELLI *et al.* 2017] that trigger accelerated soil erosion with dramatic implications for nutrient and carbon cycling, land productivity, and consequently, worldwide socio-economic conditions [KEESSTRA *et al.* 2016]. While exploring changes and future challenges posed by erosion in Mediterranean landscapes, GARCÍA-RUIZ *et al.* [2013] points that undergoing prevailing extreme events conditions, Mediterranean soils are particularly at high risk of erosion due to intensive interaction between climate, topography, soil characteristics, and human activity. In Morocco, soil erosion by water threatens nearly 75% of cropland areas and is considered as the major driver of dams' siltation [SCHILLING *et al.* 2012]. The latter leads to a yearly water loss of nearly 70 mln m<sup>3</sup> resulting in a yearly decrease of national storage capacity by 0.5% [ABDELLAOUI *et al.* 2002]. For these reasons, since the early 1960s, Morocco has been committed to a wise process of surface water mobilisation by building several dams to mitigate continuous decrease in rainfall and the frequent floods due to climate change [GOURFI *et al.* 2020].

Numerous studies have been led to estimate annual soil losses due to water erosion at the watershed level [LAHLOU *et al.* 2015]. Along with other studies, they all reported that anthropogenic activities, such as land mismanagement, deforestation, and overgrazing, are the main factors of the observed land degradation in the whole Moroccan territory [MARKHI *et al.* 2019]. These losses are mainly related to human induced land degradation that reaches high levels in the Rif mountains (24–140 t·ha<sup>-1</sup>·y<sup>-1</sup>) [ABDELLAOUI *et al.* 2002].

Considered as one of the five major Moroccan rivers regarding flow and size, the Bouregreg River is draining an area of 395,600 ha. In 1974, the Sidi Mohamed Ben Abdellah (SMBA) dam was constructed on its course to ensure water supply for a population of more than 10 million inhabitants concentrated in the big coastal cities of Casablanca and Rabat-Salé. Its initial water capacity was 446 mln m<sup>3</sup> before reaching 1,025 mln m<sup>3</sup> after the height was raised in 2006. LAOUINA and MAHÉ [2013] consider that during the last decade changes in erosive dynamics within the Bouregreg River Watershed made the SMBA dam experience huge siltation risks which are estimated to be around 2.5 Mm<sup>3</sup>·y<sup>-1</sup>, corresponding to a specific annual degradation of 370 t·km<sup>-2</sup>·y<sup>-1</sup> [LAHLOU 1986]. Numerous models are used to accurately assess local water-induced soil erosion. They can be either empirical (RUSLE) or physically-based ones, such as the Soil and Water Assessment Tool (SWAT), Water Erosion Prediction Project (WEPP), etc.

Although being worldwide used as a reliable tool of soil erosion rates, the Revised Universal Soil Loss Equation (RUSLE) model effectiveness cannot be validated in all circumstances. In fact, its use was primarily designated to be applied to some US landscapes of moderate slopes (less than 20%) where surface runoff is not the main driver of soil losses. Non-conventional sites, such as construction sites, croplands and conservation tillage fields, earned little interest regarding data gathered in both space and time. Furthermore, the RUSLE is rather parameterised

on a local scale making it unsuitable for a larger scale (regional and global). In their attempt to derive more accurate soil erosion rates at the global level using this model, they adjusted both its rainfall erosivity and topographical factors, and compared the obtained rates to those of large US and European empirical databases.

Additionally, the RUSLE model estimates only sheet and rill erosion forms with no consideration of the gully form and the dispersive soil. This leads to an underestimation of the soil loss at catchment outlets. This results in a coarse estimation of the soil losses amount delivered to dams and then of their siltation rate. Similarly, some of the RUSLE model factors are rather calculated by alternative formulas that completely differ from those established by the authors. This is mainly due to the necessity of gathering long time series data and achieving both ground truth exploratory and in-situ tests to fulfil original equations prerequisites [TANYAS *et al.* 2015].

On the other hand, temporary fluvial deposition of sediments within the eroded area before reaching the main basin waterway leads to overestimating of soil erosion rates. In Morocco, the 1970–2020 review of soil erosion modelling [MANAOUCH *et al.* 2021] indicated that the lack of meteorological stations providing long-term 30 min data and rainfall intensity measurements led RUSLE users to recourse to correlating *R* factor with available annual rainfall series. The same review is revealing that 53% of *C* factor was calculated by image classification while in 40% of studied cases, *P* factor was attributed the value of 1.

At the Mediterranean level, VAN DER KNIJFF *et al.* [1999] created a new *R* factor model that gave satisfactory results under specific climatic conditions in this region [GHOSAL *et al.* 2020]. THOMAS *et al.* [1998] indicated that a tremendous effort was done by the NRCS to calculate a new set of *C*-factor values in the whole US territory, while FERREIRA *et al.* [1995] tests demonstrated that the RUSLE is likely to be more sensitive to *C*-factor inputs. Furthermore, BRYAN [2000] qualified plots used to generate the empirical *K* factor as unsuitable to real field conditions as they do not allow the development of rills, especially in hillslopes. Given the above, the validation of the model becomes a major issue to make more accurate soil loss assessment at various scales and on-site field conditions. Such on-site validation is achieved through both the measuring of deposited sediments at the level of waterbodies and evaluation of soil losses using experimental plots to be monitored during a year. Otherwise, the use of fallout radionuclides (<sup>137</sup>Cs) becomes more common as it is cost effective and more accurate [TIAN *et al.* 2021]. FOSTER *et al.* [2003] improved the RUSLE2 model and suggested a method allowing sediment deposition integration particularly in the US highly distributed lands.

To enhance its use efficiency, the RUSLE was recently implemented along complementary models in order to take into account both sediment transport and delivery processes. KINNELL [2010] has suggested to consider integrating the runoff in the rainfall-runoff factor so as to make the RUSLE model more sensitive to spatial variations in runoff along hillslopes. Studies using the RUSLE as an empirical model for assessing soil erosion gave satisfactory reliable results. The most relevant one is that of BORRELLI *et al.* [2017], where they established the erosion “hotspots” at a global scale by assessing the effect of land use change on soil erosion over the period 2001–2012. They established then a tolerable soil loss value of 10 t·ha<sup>-1</sup>·y<sup>-1</sup> as

found that 6.1% of global soils have erosion rates exceeding this critical threshold. Regarding land use impact on such rates, they concluded that the latter range was from  $0.16 \text{ t} \cdot \text{ha}^{-1} \cdot \text{y}^{-1}$  for forests to  $12.7 \text{ t} \cdot \text{ha}^{-1} \cdot \text{y}^{-1}$  for cropland. At the European level, while using an adapted version (RUSLE2015), PANAGOS *et al.* [2015] found that erosion rates were 0.07, 3.24 and  $40.16 \text{ t} \cdot \text{ha}^{-1} \cdot \text{y}^{-1}$  in natural land cultivated soil and bare soils respectively. It revealed the obvious impact of land use/land cover on erosion severity. Subsequently, it was demonstrated that 0.4% crop yields was recorded in the same area [PANAGOS *et al.* 2015].

In the Mediterranean context, in the Mina River Watershed in Algeria, BENCHETTOUH *et al.* [2017] found that average soil losses rate was of  $11.2 \text{ t} \cdot \text{ha}^{-1} \cdot \text{y}^{-1}$ . The latter is very close to those of our case study as it is related to a catchment with similar pedoclimatic and land cover conditions. However, in the Tunisian Sourrag River Watershed, which is located in a rather more arid area, it was showed that the specific land degradation was of  $38.6 \text{ t} \cdot \text{ha}^{-1} \cdot \text{y}^{-1}$  with 58% of the watershed area affected by moderately high erosion hazard. Regarding Morocco, the specific land degradation rate ranges between 1 and  $10 \text{ t} \cdot \text{ha}^{-1} \cdot \text{y}^{-1}$  in both the Middle and High Atlas regions representing values more commonly found in a similar region of North Africa. Meanwhile, more contrasted rates are recorded in highly erosion prone mountainous part of Morocco (Rif Mountain) with losses varying from 30 to  $70 \text{ t} \cdot \text{ha}^{-1} \cdot \text{y}^{-1}$  [EL JAZOULI *et al.* 2019]. These results reveal the high sensitivity of the RUSLE model to the topographic factor, which is a measure of the sediment transport capacity of overland flow or when applied in abrupt landscapes.

Firstly, the objective of this study is to apply a mapping approach to determine major factors controlling the erosion process and influencing the sediment yield within the Bouregreg River Watershed (rainfall aggressiveness, topographic factor, soil erodibility, vegetation cover protection, soil conservation practices). Secondly, the objective is to predict the annual soil losses variation using two Landsat 8 images captured respectively in 2004 and 2019. The Revised Universal Equation of Land Losses

known as the RUSLE (Revised Universal Soil Loss Equation) was originally developed by WISCHMEIER and SMITH [1978] and it remains the most widely used model worldwide for predicting sheet and rill erosion [KIJOWSKA-STRUGALA *et al.* 2018]. This equation is supported by more than four decade experience and field surveys making it a suitable tool for erosion assessment in various landscapes, especially in agricultural lands. This model was combined to remote sensing and integrated into the Geographical Information System (GIS) to assess the basin vulnerability to water erosion hazards and quantify soil losses for 2004 and 2019. Results obtained are presented in a map that highlights water erosion hotspots corresponding to priority areas. The ultimate objective is to provide a strategic tool for land managers and policy makers to adopt suitable soil conservation measures aiming at a sustainable soil management (SSM).

In order to establish a socio-economic appraisal of soil erosion at the watershed level, a spatial distribution poverty analysis was drawn to establish the link between local population livelihoods and soil erosion severity.

## MATERIALS AND METHODS

### STUDY AREA

The Bouregreg River Watershed is a major sub-basin of the whole Bouregreg basin. It originates from the Middle Atlas Mountain and pours into the Sidi Mohamed Ben Abdellah dam (SMBA) reservoir south-east of the Rabat City. It is limited in the east by the Beht River Watershed, in the west by the Grou River sub-basin, and in the south by the High Oum Er-Rbia Watershed. In the North, it is bounded by its outlet (SMBA dam). The drained area is about 396,000 ha that is mainly made up of impermeable hills and tablelands with gentle slopes and a fairly high vegetative cover. Altitudes are significantly contrasting; they vary from 60 m downstream the catchment to 1627 m in the upstream part within the Middle Atlas Mountain (Jbel Mzourgane) (Fig. 1).

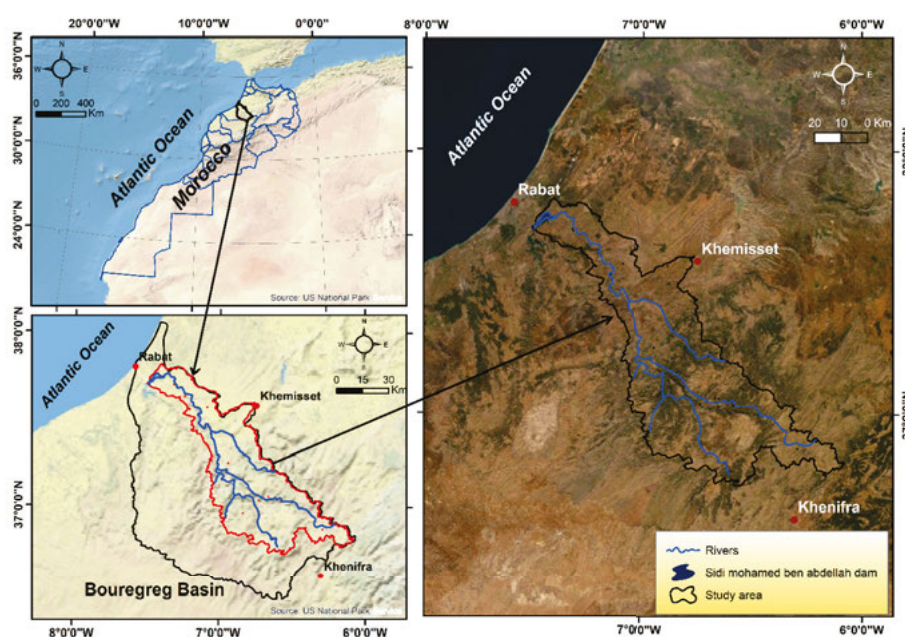


Fig. 1. The Bouregreg River watershed; source: own elaboration

The average annual rainfall ranges between 400 and 800 mm due to the various landscapes characterising the basin. The period of March–May records rainfall from 30 to 60 mm. Rainy months extend from December to February with average monthly rainfall ranging from 71 to 79 mm. The summer season (July–September) along with June are the driest periods with rainfall less than  $14 \text{ mm} \cdot \text{month}^{-1}$ . Time of concentration ( $t_c$ ) can reach 9.3 h and maximum flow is of  $810 \text{ m}^3$ , which can result in high flooding hazards especially during stormy events.

The Bouregreg River has five tributaries comprising a very hierarchical hydrological network. Consequently, the watershed is subdivided into five sub-basins: Tabahart River, Ksiksou River, Aguenour River, low Bouregreg, and middle Bouregreg (Fig. 2).

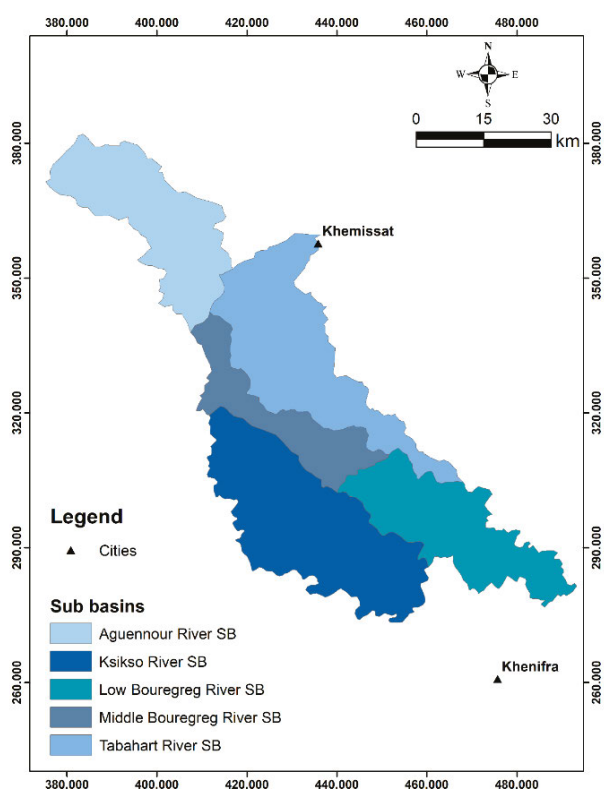


Fig. 2. Bouregreg River Watershed sub-basins; source: own elaboration

Dominant lithological formations are shale, flysch, and calcareous crusts [BEAUDET 1969]. They subdivide the watershed into four major geomorphological units from the south to the north, namely: eastern depression, highland, intermediate stratum, and the lower stratum. According to [BEAUDET 1969], the high part is characterised by brown Mediterranean soils while on the borders we can find red Mediterranean soils, vertisols, isohumic soils as well as hydromorphic ones. The main soil types that can be distinguished within the watershed area are: fersiallitic soils, lithosols, regosols, vertisols, sandy, and rough alluvial soil. Accordingly, the vegetation cover is abundant and very diversified and consists of grassland, scrubs, bushes, and woodland.

## METHODS

Since a direct field assessment of soil erosion is not often economically and technically affordable, several models have been developed as cost effective means to perform such estimation.

They endeavour to faithfully represent the landscape where the erosion process takes place by putting emphasis on the erosion physical drivers and processes. They are used in soil erosion and sediment yield prediction, in adoption of site-specific water and soil conservation measures, and in designing best management practices (BMPs) for differentiated landscape contexts. Still, the first expected objective solution is to quantify the vegetation cover and crop rotation impact on soil erosion. In this perspective, attempts to determine other factors contributing to soil erosion began from the early 1930s. Thereafter, several researchers have determined empirical equations for predicting soil losses [WISCHMEIER, SMITH 1965; 1978]. All these equations estimate the annual soil loss per unit area ( $\text{t} \cdot \text{ha}^{-1} \cdot \text{y}^{-1}$ ) with common variables: slope gradient (%), slope length (m), rain erosivity and in some cases, parameters related to both slope and length when erosion begins [MEYER 1965].

The Revised Universal Equation of Land Losses known as the RUSLE is a soil loss assessment model that calculates the potential long-term average annual soil loss at the field scale. It can also be used in farm planning by determining the most suitable crop and management systems. However, its use declined as a conservative measure. The RUSLE uses the same basic structure with the factorial approach as that of the USLE. Yet, the individual factors were calculated with algorithms that were significantly changed (Eq. 1):

$$A = R \cdot K \cdot LS \cdot C \cdot P \quad (1)$$

where:  $A$  = potential long-term average annual soil loss ( $\text{t} \cdot \text{ha}^{-1} \cdot \text{y}^{-1}$ ),  $R$  = rainfall and runoff erosivity index ( $\text{MJ} \cdot \text{mm} \cdot \text{ha}^{-1} \cdot \text{h}^{-1} \cdot \text{y}^{-1}$ ),  $K$  = soil erodibility factor ( $\text{t} \cdot \text{h} \cdot \text{MJ}^{-1} \cdot \text{mm}^{-1}$ ),  $LS$  = slope length and steepness factor;  $C$  = cover management factor,  $P$  = conservation practices' factor.

Integrated to the GIS environment, this empirical equation enables to model and assess soil losses due to rill and interrill erosion. It is a multiplicative function representing the main erosion factors in such a manner that it tends to zero whenever one of its variables approaches the null value. The study methodology chart is shown in Figure 3.

Initially originating in the USA, the RUSLE equation was further adapted to fit specific European conditions. BORRELLI *et al.* [2017] used a new version of the RUSLE known as the RUSLE2015 model. The latter arises from huge standardised European datasets gathered by the Joint Research Centre of the European Commission.

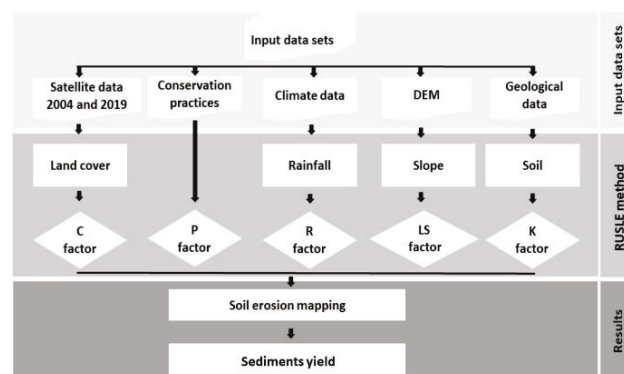


Fig. 3. Workflow chart of the study; source: own elaboration

The map resulting from the integration of all the model factors expresses the average annual losses at any point in the basin in  $t \cdot ha^{-1} \cdot y^{-1}$ . This map is of great use in locating erosion prone areas and serves as a basic document for the identification of priority areas. It also represents a valuable cartographic document for a planner to design and plan appropriate layouts.

#### • Rainfall erosivity factor ( $R$ )

Erosivity is the rain potential ability to produce erosion. It is the product of rain kinetic energy and rain maximum intensity for 30 minutes [WISCHMEIER, SMITH 1978]. It can also be considered as the average annual index of erosion by rain. Because kinetic energy and rainfall intensity data are difficult to obtain, alternative formulas requiring only monthly and annual data for determining the  $R$  factor have been developed [RANGO, ARNOLDUS 1987]. To estimate this factor, we applied the formula of RANGO and ARNOLDUS [1987] (Eq. 2) to 24 stations located in the Bouregreg River catchment over a period of 30 years (1985–2015).

$$\log R_e = 1.74 \log \left( \frac{P_i^2}{P} \right) + 1.29 \quad (2)$$

where:  $R_e$  = rain aggressiveness index (units per year),  $P_i$  = average monthly rainfall for month  $i$  (mm),  $P$  = average annual rainfall for the observation period (mm).

The  $R$  factor was calculated separately for each station and results were then generalised using the ArcGIS Kriging interpolation method to obtain the erosion factor map for the whole watershed area.

This interpolation method is used as the input data comes from a continuous phenomenon in space (rainfall measurements). The ordinary kriging was chosen as a simple prediction method (no drift). It stems from the assumption of a constant mean. Thus, it assumes the following model:

$$Z(s) = \mu + \varepsilon(s) \quad (3)$$

where:  $Z(s)$  = variable of interest for the location  $s$  (rainfall erosivity),  $\varepsilon(s)$  = spatially correlated stochastic part of variation,  $\mu$  = constant stationary function (global mean).

Then default parameter values determined by the wizard was used to calculate the kriged estimates.

#### • Soil erodibility factor ( $K$ )

The soil erodibility factor is the description of the soil intrinsic characteristics. Erodibility is affected both by soil properties (infiltration rate, permeability, particle dispersion) and by the raindrop splash effect.

Factor  $K$ , which is defined as the amount of soil lost per unit area under certain standard conditions, can be calculated using different formulas. It explains the influence of soil ownership on soil losses during rainy events.

The  $K$ -factor values were obtained through the nomograph of WISCHMEIER and SMITH [1978] applied to the pedological map of the study area on the scale of 1:500,000 along with soil analysis of field samples and similar studies results.

The equation to calculate  $K$  values is expressed as follows (Eq. 4):

$$100K = 2.1M^{1.14} \cdot 10^{-4} (12 - OM) + 3.25(S - 2) + 2.5(P - 3) \quad (4)$$

where:  $K$  = soil erodibility factor ( $t \cdot ha \cdot MJ^{-1} \cdot mm^{-1}$ ),  $M$  = (% silt + % fine sand)  $\cdot$  (100 - % clay),  $OM$  = % of organic matter,  $S$  = soil structure code,  $P$  = permeability code.

The code values for permeability ( $P$ ) are: 1: rapid to very rapid permeability, 2: moderately rapid permeability, 3: average permeability, 4: moderately slow permeability, 5: slow permeability, 6: very slow permeability. The code values for the soil structure code ( $S$ ) are: 1: very fine grain size (<1 mm), 2: fine particle size (1–2 mm), 3: medium (2–5 mm) to coarse (5–10 mm) grain size, 4: very coarse grain size (>10 mm).

Each homogeneous unit is assigned the value of  $K$  which corresponds to it.

#### • Topographic factor ( $LS$ )

The most important relief parameters that determine the water erosion intensity are the slope gradient and length. These two factors have a key role in increasing water erosion of soils. The steeper slope, the more soil erosion will be caused by water. Water erosion also increases with the length of the slope due to the increase in runoff.

The topography parameter is calculated from digital elevation model images (DEM) of the Shuttle Radar Topography Mission (SRTM) with a resolution of 30 m, downloaded from the US Geological Survey (<https://earthexplorer.usgs.gov>). The ArcGis software greatly facilitated the calculation of certain parameters, such as the topographic factor, which was calculated from the DEM, the slope class map, and the flow map according to the following expression by WISCHMEIER and SMITH [1978] (Eq. 5):

$$LS = [(L/22.15)^m] [(65.41 \sin^2(S) + 4.56 \sin(S) + 0.065)] \quad (5)$$

where:  $L$  = slope length (m),  $S$  = slope steepness (%),  $m$  = factor which depends on the value of  $S$ .

$$S \geq 5\% \rightarrow m = 0.5$$

$$3.5\% \leq S < 5\% \rightarrow m = 0.4$$

$$1\% \leq S < 3.5\% \rightarrow m = 0.3$$

$$S < 1\% \rightarrow m = 0.2$$

Slope length ( $L$ ) is defined as the distance from the point of origin of overland flow to the point where either the slope gradient decreases enough that deposition begins or the runoff water enters a well-defined channel that may be part of a drainage network or a constructed channel.

VAN REMORTEL *et al.* [2004] developed a slope length calculation algorithm that was revised by ZHANG *et al.* [2013]. This cell-based method is expressed as follows:

$$\lambda_{i,j} = A_{i,j-out} / D_{i,j} \quad (6)$$

where:  $A_{i,j-out}$  is the contributing area at the outlet of grid cell with coordinates  $i, j$  ( $m^2$ ),  $D_{i,j}$  = effective contour length of coordinates  $i, j$  (m),  $\lambda_{i,j}$  = slope length of coordinates ( $i, j$ ) (m).

#### • Cover factor ( $C$ )

The cover management factor ( $C$ ) integrates the influence of plant cover, yield level, and cultural practices and it is often used to assess the effect of land management methods on erosion. It is the reduction factor that has the largest impact on erosion. It represents the ratio between soil losses under a given land condition to that of the unit fallow plot which has been plowed in the greatest slope direction and has not received input organic matter for at least three years, at which index  $C = 1$  is assigned [WISCHMEIER, SMITH 1978].

Remote sensing data were used to calculate  $C$  factor. It consists of a supervised classification technique of two Landsat 8



images, downloaded from the US Geological Survey (<https://earthexplorer.usgs.gov>) and acquired in 2004 and 2019 to assess the land use change effect on the annual soil loss in the watershed. The formula used to determine  $C$  factor using the Normalized Difference Vegetation Index ( $NDVI$ ) providing information on vegetative cover and its health is that of VAN DER KNIJFF *et al.* [1999] (Eq. 7):

$$C = \exp\{-[\alpha NDVI / (\beta - NDVI)]\} \quad (7)$$

where:  $\alpha$  and  $\beta$  = unitless parameters which determine the curve shape connecting  $NDVI$  to  $C$  factor.

In this equation, the values 2 and 1 were assigned respectively to  $\alpha$  and  $\beta$ . This equation is more accurate than the linear relationship [VAN DER KNIJFF *et al.* 1999] and it has been used successfully under similar soil and climatic conditions within the semi-arid N'fis basin (High Atlas, Morocco) [MARKHI *et al.* 2019].

#### • Supporting practices factor ( $P$ )

Additionally, factor  $P$  expresses the ratio of soil losses by water erosion for a given type of anti-erosive practice to that obtained on a soil with straight row farming up-and-down slope and devoid of any anti-erosive measure [WISCHMEIER, SMITH 1965].

The adoption of soil erosion control and prevention measures can considerably meet many the United Nations' Sustainable Development Goals (UN SDGs) which are namely: SDG 2 "Zero hunger", SDG 3 "Good health and wellbeing", SDG 6 "Clean water & sanitation", SDG 13 "Climate action", and SDG 15 "Life on land".

To address soil erosion issue worldwide, the FAO released the Voluntary Guidelines for Sustainable Soil Management which identify four sub-sets of soil conservation measures.

Since our field survey revealed that no significant soil conservation measures are in use (terracing, contouring, strip cropping, grassed waterways, etc.), the  $P$  factor was assigned the value of 1 for the whole watershed drainage area [CHUENCHUM *et al.* 2020].

## RESULTS AND DISCUSSION

### CLIMATE AGGRESSIVENESS FACTOR $R$

In the estimation of the soil erosion rate variation, the daily rainfall is an appropriate indicator to characterise the seasonal distribution of sediment yield. Hence, the major part of soil loss happens during the rainy season, especially in extreme events such as major storms.

Average annual rainfall related data enable to characterise both wet and dry periods depending on their series continuity. It shows that values vary significantly from station to another and range from 400 to 800 mm (Tab. 1).

Depending on their respective elevation, the watershed stations are classified, in a descending order into rainy ones ( $>500 \text{ mm}\cdot\text{y}^{-1}$ ): El Harcha, Oulmes, Moulay Bouazza, Maaziz, Dar Laaroussi, Bir Ameur, Tifoughaline, Timeskaouine and Sidi Ahssine. Low rainfall ones ( $<400 \text{ mm}\cdot\text{y}^{-1}$ ) are those of Ain Harrak, Ain Harcha, Lalla Chafia, and Sidi Amar.

After calculating  $R$  factor for the 24 watershed stations, the  $R$  factor map was derived using the Kriging interpolation tool. The  $R$  factor values range from 65 to 105  $\text{MJ}\cdot\text{mm}\cdot\text{ha}^{-1}\cdot\text{y}^{-1}$  (Tab. 2)

**Table 1.** Stations' rainfall characteristics

Station	Elevation (m a.s.l.)	Average yearly rainfall ( $\text{mm}\cdot\text{y}^{-1}$ )
Aguibat Ezziar	90	417
Ain Harrak	400	392
Ain Kohel	630	401
Ain Labiod	971	492
Ain Harcha	267	414
Bir Ameur	150	512
Boukhmis	900	466
Dar Laaroussi	827	589
El Harcha	890	797
Lalla Chafia	180	360
Maaziz	220	526
My Bouazza	1070	563
Moumou	960	500
Oulmes	1050	773
Sidi Ahsine	1200	603
Sidi Allal El Behraoui	178	501
Sidi Amar	240	387
SMBA	148	463
Souk Sebt Ait Ikkou	335	452
Tiflet	320	529
Tifoughaline	1259	578
Timeskaouine	750	562
Tsalat	630	458
Tiddas	450	478

Source: own elaboration based on National Center for Forest Research Rabat data.

corresponding to a high level of rainfall aggressiveness within the whole watershed area. The  $R$  factor spatial variation indicates a gradient notable decrease from the South-East to the North-West of the basin following the altitude gradient patterns. It comes out that 54% of its total drainage area is under a high climatic aggressiveness with  $75 < R$  (Fig. 4).

The  $R$  values are close to those obtained in neighbouring watersheds with a notable rainfall spatio-temporal irregularity.

**Table 2.** Climatic aggressiveness classes in the Bouregreg River Watershed

$R$ factor value ( $\text{MJ}\cdot\text{mm}\cdot\text{ha}^{-1}\cdot\text{y}^{-1}$ )	Aggressiveness classes ( $R$ )	Area (ha)	% of total area
$<65$	very high	2,741	0.69
[65–75[	high	181,430	45.86
[75–85[	medium	112,976	28.56
[85–95[	low	61,172	15.46
[95–105[	very low	37,281	9.42
Total		395,600	100.00

Source: own elaboration.

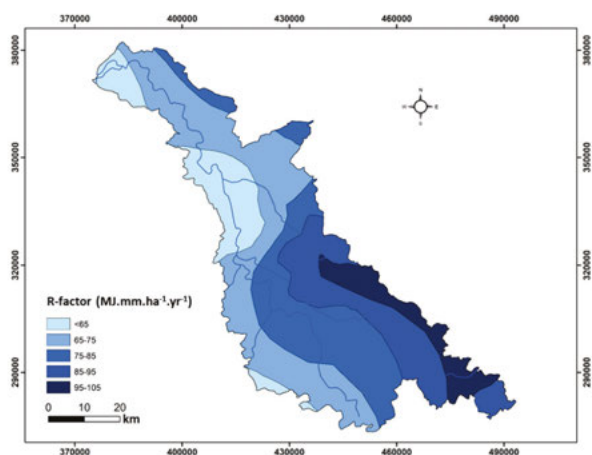


Fig. 4. Rain erosivity factor  $R$  map of the Bouregreg River Watershed; source: own study

YJJOU *et al.* [2014] reported that 93% of the High Oum Er-Rbia basin area is subject to an erosivity with  $R$  values varying from 70 to 119 while the remaining area (7%) undergoes low erosion risk. AIT YACINE *et al.* [2019] indicated that in Beht watershed, the rainfall aggressiveness  $R$  values range between 65.0 and 127.5.

### SOIL ERODIBILITY FACTOR $K$

The importance of the different soil types distribution in the watershed is illustrated by Figure 5. This distribution shows a dominance of little evolved soils which cover 40.6% of the basin area followed by complex C2 and C1 soil units. The latter occupy, respectively, 17.5 and 16.6% of the total area. They are located mainly in rugged parts of the basin and generally evolve under forest vegetation. These soils exhibit significant variations at short distances and are subject to almost permanent erosion.

As shown in Table 3, at the watershed level, soil erodibility factor values vary from 0.25 to  $0.65 \text{ t}\cdot\text{ha}\cdot\text{MJ}^{-1}\cdot\text{mm}^{-1}$ . In fact, 60% of the watershed total area is covered by erosion prone soils with  $K$  values oscillating from 0.45 to 0.65. Very high erodibility soils

( $K > 0.65$ ) occupy 11,351 ha corresponding to 2.87% of the total area, while high protection can only be seen on 10.8% of the catchment area. These values indicate a prevailing high lithological fragility within the basin (Fig. 6).

Unlike clay soils, due to their high infiltration rates generating less runoff, silty soils are less resistant to detachment due to their high infiltration rates and then are easily transported [GASHAW *et al.* 2020]. Low erodibility is often observed on vertisols ( $0.1 < K < 0.2$ ), whereas poorly developed soils are linked to high  $K$  values ( $> 0.4$ ). These results sound logical as the lower  $K$  factor values are those of the soils characterised by low permeability and low antecedent moisture content.

Elsewhere, a strong correlation ( $-77\%$ ) between  $K$  factor values and permeability was established while determining erodibility factor  $K$  in the Dembecha Watershed, Northwest Ethiopia [OSTOVARI *et al.* 2017]. In the high Oum Er-Rbia Watershed, results show that 59% of soils have a very high erodibility between 0.4 and 0.5, whereas only 22% of the surface of the basin has a low erodibility of less than 0.2 [YJJOU *et al.* 2014]. In the adjacent Beht watershed, 89.27 % of the basin area has high soil erodibility factor ranging from 0.3 to 0.67 [AIT YACINE *et al.* 2019].

Table 3. Erodibility factor ( $K$ ) classes in the Bouregreg River Watershed

$K$ factor value ( $\text{t}\cdot\text{ha}\cdot\text{MJ}^{-1}\cdot\text{mm}^{-1}$ )	$K$ factor class	Area (ha)	% of total area
<0.25	very low	13,281	3.36
[0.25–0.35[	slightly low	29,471	7.45
[0.35–0.45[	low	117,230	29.63
[0.45–0.55[	medium	169,043	42.73
[0.55–0.65[	high	55,224	13.96
>0.65	very high	11,351	2.87
Total		395,600	100.00

Source: own study.

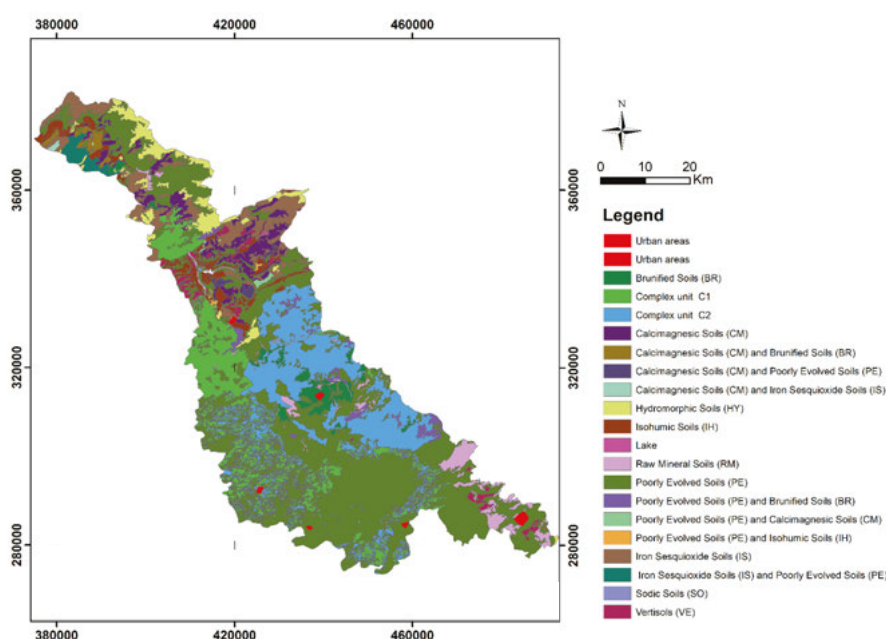


Fig. 5. Pedological map of Bouregreg River Watershed; source: own study

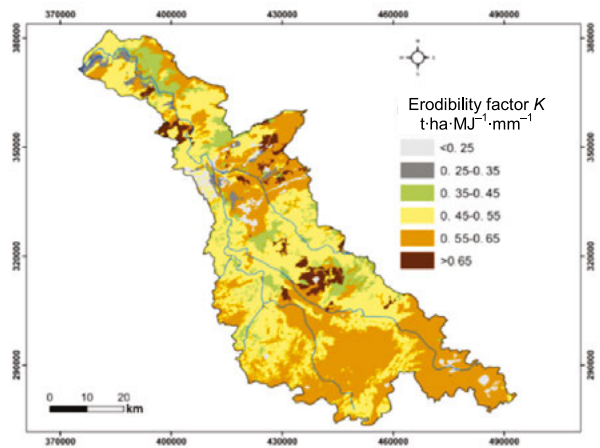


Fig. 6. Erodibility factor  $K$  map of the Bouregreg River Watershed; source: own study

### TOPOGRAPHIC FACTOR ( $LS$ )

The  $LS$  factor reflects both slope length and steepness effect on the erosion process across the watershed. Its distribution map was obtained using a DEM with a spatial resolution of 20 m. Five classes of the topographic factor were distinguished with values ranging from 0.1 to 41 with an average value of 8.3 (Tab. 4). The watershed area is dominated by  $LS$  classes with values beneath 20 (75%). Classes with the highest  $LS$  values (20–30 and >30) corresponding to the rugged parts of the basin occupy

Table 4. Classes of topographic factor ( $LS$ ) in the Bouregreg River Watershed

$LS$ factor value	$LS$ factor class	Area (ha)	% of total area
<5	very gently sloping	181,230	45.81
[5–15[	gently sloping	67,850	17.15
[15–20[	moderately sloping	47,320	11.96
[20–30[	moderately steeply sloping	57,370	14.50
>30	steeply sloping	41,830	10.57
<b>Total</b>		<b>395,600</b>	<b>100.00</b>

Source: own study.

respectively 14.50 and 10.57% of the total drainage area. Thus, the basin can be considered as generally dominated by moderate to steep slope landscapes resulting in a high erosion hazard. The spatial variability shows a decreasing gradient from the South-East to the North-West (Fig. 7). According to the results, we can conclude that topographic factor  $LS$  values decrease as the flow accumulation and slope decrease too.

By contrast, at the contiguous watershed of Beht, 87.8% of the surface has a relatively low  $LS$  factor (<5). A high spatial variability is noted with  $LS$  factor values ranging between 0.44 and 125.67 [AIT YACINE *et al.* 2019]. At the High Oum Er-Rabi catchment, results showed that 62% of the catchment area is in class 5 to 30 [YJJOU *et al.* 2014].

### VEGETATION COVER ( $C$ )

To generate accurate evaluation of local soil erosion rates, the RUSLE equation needs proper value of soil cover for soils under different forms of land use and management [BIDDOCCU *et al.* 2020]. The vegetation action reflected by the  $C$  factor constitutes the most deterministic and dynamic parameter for Moroccan watersheds. The land cover map provided by the Regional Directorates of Water and Forests of the North-West and the Middle Atlas, as well as the map of land cover by vegetation (NDVI) [VAN DER KNIJFF *et al.* 1999] were used as basic documents for the  $C$  factor determination (Fig. 8). These data were compared

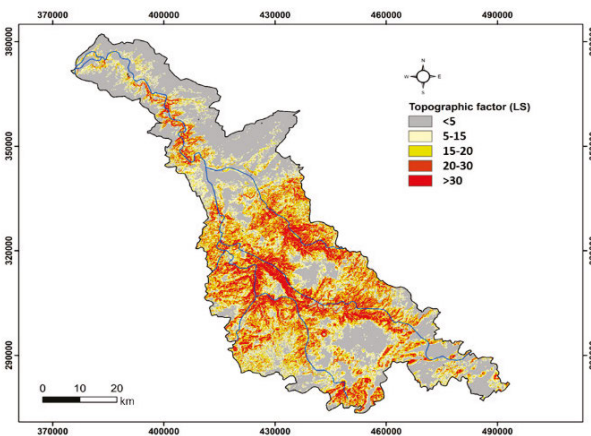


Fig. 7. Topographic factor ( $LS$ ) map of the Bouregreg River Watershed; source: own study

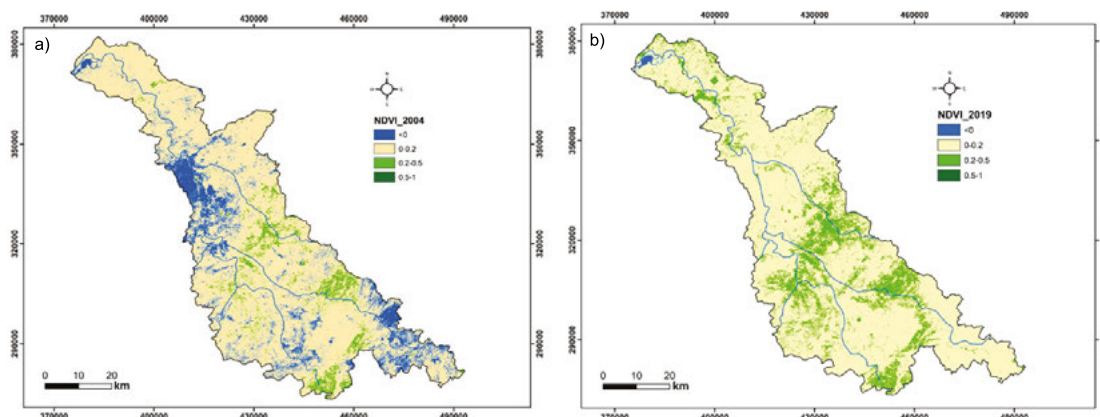


Fig. 8. Normalized Difference Vegetation Index (NDVI) map of the Bouregreg River Watershed in: a) 2004, b) 2019; source: own study



to those obtained from field inspections across representative sample locations that cover the whole study area.

The *C* factor represents the farming practices that are often used to determine the conservation soil as well as the degree of crop production. The spatial distribution map of the cover index shows that the most sensitive areas to erosion are those with low vegetation density, which mainly cover the upstream part of the watershed. Figure 9 highlights the *C*-factor distribution within the study area in 2004 and 2019 respectively.

The basin area is occupied by different land covers to which we have assigned different values of *C* factor. Bare areas are given the value of 1.0, for cropland the value is 0.70, for the grazing land 0.48, for natural shrubs 0.18, and 0.08 for dense forests (Tab. 5). Low values of *C*-factor reflect less vulnerability to erosion hazard. The higher vegetation density, the lower is the soil erosion rate. In fact, the vegetation cover provides a physical barrier to rain aggressiveness, and thus, it keeps the coarse aspect of the soil surface and improves both its chemical and physical properties [MAQSOOM *et al.* 2020]. For their part, BIDDOCU *et al.* [2020] used the ORUSCAL (Orchard RUSLE CALibration) software to identify the best soil cover and management factor (*C*) for the RUSLE in five European vineyards with different soil management patterns. It was established that among five strategies, Permanent Cover Crops (PCC) involving complete cover of the field was the only one to achieve sustainable erosion rates within the study area.

**Table 5.** Vegetation cover (*C*)-factor values assigned for each land use class in the Bouregreg River Watershed

Land use classes	Assigned <i>C</i> values	Soil protection level	Area (ha)	% of total area
Built-up areas	0	–	3,283	0.83
Wet areas	0	–	2,492	0.63
Dense forest	0.08	very high	39,995	10.11
Matorral (natural shrubs)	0.18	high	82,047	20.74
Rangeland	0.48	weak	76,193	19.26
Cropland	0.7	very weak	186,723	47.20
Bare soil	1.0	none	4,866	1.23
<b>Total</b>			<b>395,600</b>	<b>100.00</b>

Source: own study.

The spatial distribution of different *C*-factor values vary from 0 to 0.9. Low values of *C*-factor are an indicator that the area is less susceptible to the soil erosion process. Results obtained for the 2019 map show that 89% of the basin area has a very low level of vegetation cover and only 11% of the watershed area is well protected according to the *C* value distribution. The low protection class (>0.5) covers more than 2/3 of total area (Fig. 10).

A diachronic analysis of the land-use cartographic results (Tab. 6) reveals that the forests of the Bouregreg River watershed experience a 24% decline in terms of their area. Degradation of forest ecosystems is mainly due to clearing, cultivation, and overgrazing. The Matorral and the rangeland pastoral areas have experienced a spectacular increase of respectively 41% and 79%. This alarming tendency is the corollary of excessive forest exploitation due to deforestation and overgrazing. The latter is rather linked to farming and extended livestock stay within the forest. Cultivated lands recorded an increase of 11% due to climate change and drought. Such situation shows a substantial impact of rainfall on changes in the soil cover.

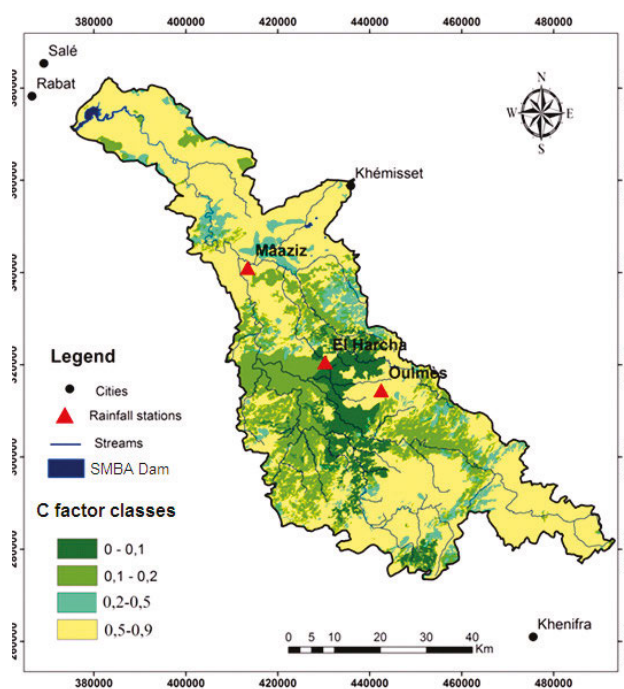


**Fig. 10.** Land cover *C*-factor map of the Bouregreg River Watershed in 2019; source: own study

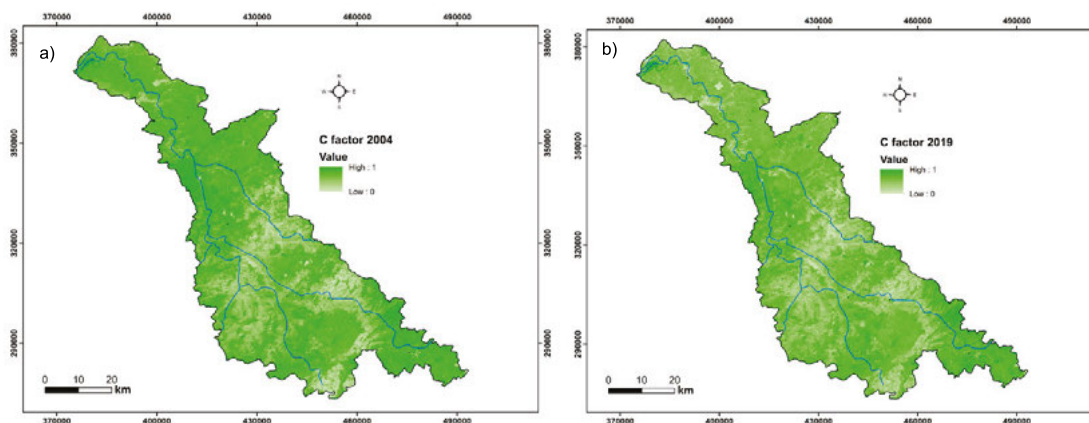


**Fig. 9.** Vegetation cover *C*-factor map of the Bouregreg River Watershed in: a) 2004, b) 2019; source: own study

**Table 6.** The evolution of land use areas in the Bouregreg River Watershed between 2004 and 2019

Land use	2004		2019		Variation (%)
	area (ha)	%	area (ha)	%	
Dense forest	156,152	40	117,803	30	-24.56
Croplands	211,548	53	235,085	59	+11.13
Mattoral (natural shrubs)	19,500	5	27,645	7	+41.77
Rangeland	8,400	2	15,067	4	+79.37
<b>Total</b>	<b>395,600</b>	<b>100</b>	<b>395,600</b>	<b>100</b>	-

Source: own study.

Obviously, in the last two decades, the Bouregreg River Watershed has experienced an increased pressure due to the impoverishment and vulnerability of local populations and their dependence on forest resources resulting in irreversible degradation of the latter. Similarly, the variation of climatic conditions (succession of drought years) has led to a regression of the vegetation cover that makes the soil more sensitive to erosion.

In the Gilgel Abay Watershed, upper Blue Nile basin, GASHAW *et al.* [2020] has showed that extensive cultivation management scenario amplify soil erosion by water. To reduce the sedimentation rate of Lake Tana, they even suggested to ban cultivation in steep slopes (>15%) by law to alleviate the ongoing soil loss. Using the CENTURY model, BALDASSINI and PARUELO [2020] analysed Soil Organic Content (SOC) changes during two decades within the semi-arid Chaco of Argentina, a region deeply affected by deforestation. He analysed combined effects of both land cover conversion from a forest system to cropland and that of land use represented by management practices within two sites. Results showed that for cropping systems there was an average reduction in SOC of 25% as compared to the native forest in 98.5% of simulations performed.

### ASSESSMENT OF SOIL LOSSES' CHANGES

Soil loss annual values were classified into five erosion vulnerability classes corresponding to five intensity levels ranging from weak (<5 t·ha<sup>-1</sup>·y<sup>-1</sup>) to extremely strong (>30 t·ha<sup>-1</sup>·y<sup>-1</sup>) [BEHERA *et al.* 2020] – Table 7.

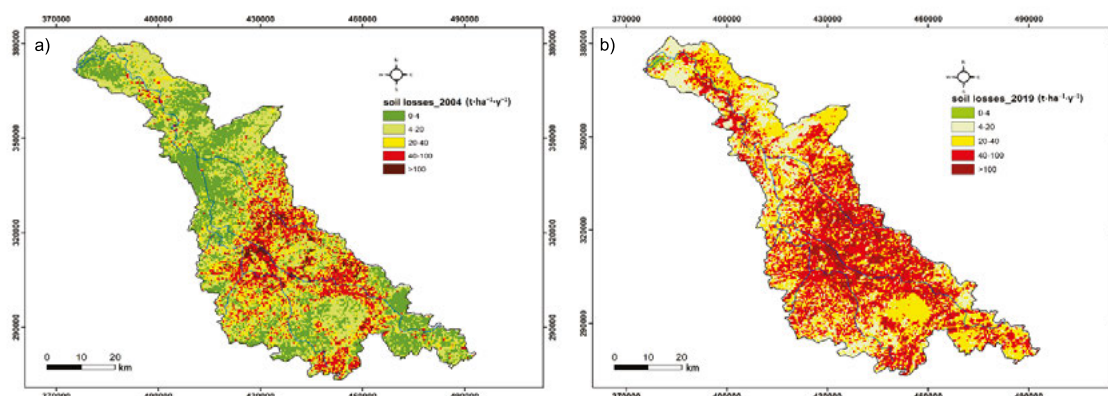
**Table 7.** Erosion class changes in the Bouregreg River Watershed between 2004 and 2019

Soil loss classes (t ha <sup>-1</sup> ·y <sup>-1</sup> )	Intens- ity	2004		2019		Gain / loss (%)
		area				
		ha	%	ha	%	
0–5	weak	181,763	45.3	45,920	11.58	–75
5–10	moder- ate	71,456	18.02	37,450	9.44	–47
10–20	strong	61,920	15.61	95,620	24.11	+54
20–30	very strong	27,637	6.97	61,370	15.47	+122
>30	extre- mely strong	52,824	13.57	155,240	39.39	+190
Total		395,600	100	395,600	100	

Source: own study.

In fact, significant changes occurred in classes (20–30) and (>30) which increased by 122% and 190 % respectively from 2004 (61,920 ha) to 2019 (95,620 ha). Meanwhile, the low soil loss classes (0–5) and (5–10) dropped down respectively by 75% (from 181,763 to 45,920 ha) and 47% (from 71,456 to 37,450 ha) during the same period. The analysis of results reveals that in 2004 64% of the watershed area was classified as exposed to weak/moderate erosion hazards with an annual soil loss rate <10 t·ha<sup>-1</sup>·y<sup>-1</sup>. This area decreased significantly to only 21% in 2019.

The factorial approach of the RUSLE model enabled to combine driving factors maps to obtain the soil loss distribution in the whole watershed area (Fig. 11). An average soil loss rate increased by 56% from 11.78 t·ha<sup>-1</sup>·y<sup>-1</sup> in 2004 to 18.38 t·ha<sup>-1</sup>·y<sup>-1</sup> in 2019 (Tab. 7). Almost 20.5% of the basin area underwent very strong to extremely strong erosion in 2004. This proportion became much higher in 2019, reaching 55%. Such strong erosion rates are exceeding the tolerated soil loss and are recorded both downstream and upstream of the Bouregreg River catchment (>30 t·ha<sup>-1</sup>·y<sup>-1</sup>). This makes the agricultural production potential severely compromised. These high rates can be explained by the fact that the upstream part of the watershed is characterised by a weak vegetative cover due to the dominance of agricultural lands which do not protect the soil effectively against the erosion hazard. High amount of sediments generated in this part

**Fig. 11.** Annual soil losses in the Bouregreg River watershed in: a) 2004, b) 2019; source: own study

can also be due to harsh weather conditions with rain aggressiveness  $R$  factor values exceeding 85 and a high soil vulnerability ( $K > 0.55$ ) (ferrallitic, calcimagnetic, and poorly developed). Still, these rates are of less importance as compared to those recorded in the Northern Rif area ( $30\text{--}70\text{ t}\cdot\text{ha}^{-1}\cdot\text{y}^{-1}$ ) [IBRAHIMI *et al.* 2005]. On the other hand, in the central part of our study area, soil losses are relatively low as weakly erodible soils with high clay percentage are dominant, e.g. vertisols ( $K < 0.2$ ). These results are consistent with findings from the High Oum Er-Rbia Watershed [YJJOU *et al.* 2014].

Using  $^{137}\text{Cs}$  and  $^{210}\text{Pb}_{\text{ex}}$  as radioisotopic soil tracers, BENMANSOUR *et al.* [2013] estimated erosion rates under Mediterranean conditions, respectively  $14.3$  and  $12.1\text{ t}\cdot\text{ha}^{-1}\cdot\text{y}^{-1}$ . These were close to those of our study area, in a crop land located in the Marchouch area, Rabat, Morocco. In the M'dez watershed (upper Sebou, Middle Atlas, Morocco) average soil losses obtained by both SWAT and RUSLE were estimated at  $3.95$  and  $2.94\text{ t}\cdot\text{ha}^{-1}\cdot\text{y}^{-1}$  respectively [BOUFALA *et al.* 2020].

In a typical Mediterranean environment (Portofino promontory, NW-Italy), RELLINI *et al.* [2019] obtained an annual soil loss mean value of  $9\text{ t}\cdot\text{ha}^{-1}\cdot\text{y}^{-1}$  whereas the tolerable one is estimated at  $11\text{--}12\text{ t}\cdot\text{ha}^{-1}\cdot\text{y}^{-1}$ . It was also found that only one quarter of the studied area showed a soil loss value that exceeded sustainable soil loss threshold.

At the European scale, PANAGOS *et al.* [2015a] applied a modified RUSLE model (RUSLE2015) taking 2010 as a reference year and obtained a mean value of  $2.46\text{ t}\cdot\text{ha}^{-1}\cdot\text{y}^{-1}$  leading to a total annual soil loss of 970 Mt.

From 2004 to 2019, low Bouregreg, Ksiksou River and middle Bouregreg sub-basins have witnessed the highest variation in terms of average soil losses,  $+85.37$ ,  $+66.06$  and  $+51.55\%$  respectively. These variations can be explained by a sudden shift from forest and range areas to cropland systems (low Bouregreg) and by the dominance of steep slopes within the landscape and dropping forest cover (low Bouregreg). These findings were confirmed with Google Earth and by several field visits to the whole catchment area. The respective contribution in sediment yield was linearly proportional to each sub-basin area. Nevertheless, to determine priority sub-basins, we considered the average soil losses ( $18.38\text{ t}\cdot\text{ha}^{-1}\cdot\text{y}^{-1}$ ) recorded in 2019. Thus, regarding the emergency of implementing appropriate Soil and Water Conservation measures by decision makers, the ranking

brought out the Ksiksou River, the Tabahart River, and Low Bouregreg sub-basins with respectively  $21.82$ ,  $20.77$  and  $19.76\text{ t}\cdot\text{ha}^{-1}\cdot\text{y}^{-1}$  as shown in Table 8.

This qualitative erosion assessment within the Bouregreg River basin corroborate the fact that in areas with rugged field, accelerated soil losses remain high even if they are covered with strictly protected vegetation. As confirmed by [EL JAZOULI *et al.* 2019] in the High Oum Er-Rbia Watershed, this topographic fragility ( $LS > 20$ ) is further exacerbated by the lithological softness of weakly compacted soils, such as marls, schist, and flyschs.

Soil losses rates in 2019 are compatible with those found by [HARA *et al.* 2020] at the scale of the whole Bouregreg watershed, which were estimated at around  $20\text{ t}\cdot\text{ha}^{-1}\cdot\text{y}^{-1}$ . Meanwhile, in her research findings, CLARK [2015], who discussed the implication of soil losses on water planning and land management, found rates exceeding  $25\text{ t}\cdot\text{ha}^{-1}\cdot\text{y}^{-1}$  at the level of the same watershed.

## CONCLUSIONS

This study unveiled the high accuracy of an appropriate combination of GIS and remote sensing techniques in assessing land use/land cover changes at the watershed level from 2004 to 2019. The erosion risk evaluation in Bouregreg River basin was further carried out using the Revised Universal Equation for Soil Loss (RUSLE). Driving factors ( $R$ ,  $K$ ,  $LS$ ,  $C$  and  $P$ ) involved in erosion processes have been determined together with their overlaying maps in the GIS environment. This led to the establishment of a soil losses distribution map for the basin.

The study area has highly aggressive climatic conditions, since 54% of its total area shows high rainfall aggressiveness factor values ( $75 < R$ ). Erosion prone soils with ( $0.45 < K < 0.65$ ) represent 60% of the watershed total area. This reflects the high lithological susceptibility of soils to erosion. Topographic factor  $K$  values range from 0.1 to 41, with an average of 8.3. This makes the basin dominated by moderately steep slopes. The highest values correspond to hilly parts ( $K > 20$ ) where erosion prevails.

Anthropogenic activities are the main cause behind land use changes over the study period (2004–2019). They led to shrinking forests areas, cropland sprawl in erosion prone soils, and highly degraded lands abandoned along steep slopes with varied

**Table 8.** Soil losses' changes by sub-basin (from 2004 to 2019)

Sub-basin	Area (ha)	2004		2019		Average soil losses' variation (%)	Ranking by priority
		average soil losses	total losses	average soil losses	total losses		
		t·ha <sup>-1</sup> ·y <sup>-1</sup>					
Ksiksou River	110,700	13.14	1,454,915	21.82	2,415,258	+66.06	1
Tabahart River	94,850	15.30	1,450,875	20.77	1,970,499	+35.75	2
Low Bouregreg	70,830	10.66	754,783	19.76	1,399,713	+85.37	3
Middle Bouregreg	44,040	9.06	399,090	13.73	604,616	+51.55	4
Aguennour River	75,180	7.99	600,827	11.72	881,456	+46.68	5
Watershed	395,600	11.78	4,660,490	18.38	7,271,541	+56.02	

Source: own study.

responses in terms of soil erosion potential in sub-basins. Consequently, the most obvious positive changes in erosion hazards were noticed in areas that witness an increase in agriculture and highly degraded areas or those under a high pressure on natural resources, such as forests and pasturelands. Over the study period, the overall impact of LULC changes resulted in a noticeable increase in the average erosive potential within the whole watershed area from  $11.78 \text{ t}\cdot\text{ha}^{-1}\cdot\text{y}^{-1}$  (2004) to  $18.38 \text{ t}\cdot\text{ha}^{-1}\cdot\text{y}^{-1}$  (2019) with varied responses according to the site-specific weather and topographic conditions. At the sub-basin level, the Ksiksou River, the Tabahart River, and low Bouregreg sub-basins recorded the highest average soil losses in 2019 with respectively 21.82, 20.77 and  $19.7 \text{ t}\cdot\text{ha}^{-1}\cdot\text{y}^{-1}$ , which corresponded (from 2004) to variations of +66.06, +35.75, and +85.37 % respectively. Thus, they are considered as the first ranked areas in terms of emergency response. Furthermore, the analysis of autochthon rural population socio-economic conditions based on the General Census of population and housing data showed that their income level is a key factor in exacerbating the erosion phenomenon across the watershed. High human pressure on natural resources due to deforestation and overgrazing is highly linked to low local population income levels (<20,000 per household per year). Such relevant results can support an urgent and targeted intervention in these priority areas through a package of integrated appropriate Soil and Water Conservation measures and living conditions enhancement aiming at a more sustainable land management to meet the UN 2030 Sustainable Development Goals (SDGs).

## REFERENCES

- ABDELLAOUI B., MERZOUK A., ABERKAN M., ALBERGE J. 2002. Bilan hydrologique et envasement du barrage Saboun (Maroc) [Hydrological balance and siltation of the Saboun dam (Morocco)]. *Revue des sciences de l'eau / Journal of Water Science*. Vol. 15(4) p. 737–748. DOI 10.7202/705478ar.
- AIT YACINE E., OUDJIA F., NASSIRI L., ESSAHLAOUI A. 2019. Modeling and mapping of soil water erosion risks through the application of GIS, Remote Sensing and PAP/RAC guidelines. Case of Beht Watershed, Morocco. *European Scientific Journal*. Vol. 15(12), 259. DOI 10.19044/esj.2019.v15n12p259.
- BALDASSINI P., PARUELO J.M. 2020. Deforestation and current management practices reduce soil organic carbon in the semi-arid Chaco, Argentina. *Agricultural Systems*. Vol. 178, 102749. DOI 10.1016/j.agsy.2019.102749.
- BEAUDET G. 1969. Le plateau central marocain et ses bordures: étude géomorphologique. The Moroccan central plateau and its borders: geomorphological study. Rabat. French and Moroccan Printing House pp. 478.
- BEHERA M., SENA D.R., MANDAL U., KASHYAP P.S., DASH S.S. 2020. Integrated GIS-based RUSLE approach for quantification of potential soil erosion under future climate change scenarios. *Environmental Monitoring and Assessment*. Vol. 192(11) p. 1–18. DOI 10.1007/s10661-020-08688-2.
- BENCHETTOUH A., KOURI L., JEBARI S. 2017. Spatial estimation of soil erosion risk using RUSLE/GIS techniques and practices conservation suggested for reducing soil erosion in Wadi Mina watershed (northwest, Algeria). *Arabian Journal of Geosciences*. Vol. 10, 79. DOI 10.1007/s12517-017-2875-6.
- BENMANSOUR M., MABIT L., NOUIRA A., MOUSSADEK R., BOUKSIRATE H., DUCHEMIN M., BENKAD A. 2013. Assessment of soil erosion and deposition rates in a Moroccan agricultural field using fallout  $^{137}\text{Cs}$  and  $^{210}\text{Pb}_{\text{ex}}$ . *Journal of Environmental Radioactivity*. Vol. 115 p. 97–106. DOI 10.1016/j.jenvrad.2012.07.013.
- BIDDOCCU M., GUZMAN G., CAPELLO G., THIELKE T., STRAUSS P., WINTER S., ..., GÓMEZ, J.A. 2020. Evaluation of soil erosion risk and identification of soil cover and management factor (C) for RUSLE in European vineyards with different soil management. *International Soil and Water Conservation Research*. Vol. 8(4) p. 337–353. DOI 10.1016/j.iswcr.2020.07.003.
- BORRELLI P., ROBINSON D.A., FLEISCHE, L.R., LUGATO E., BALLABIO C., ALEWELL C., ... PANAGOS P. 2017. An assessment of the global impact of 21st century land use change on soil erosion. *Nature Communications*. Vol. 8(1) p. 1–13. DOI 10.1038/s41467-017-02142-7.
- BOUFALA M., EL HMAIDF A., CHADLI K., ESSAHLAOUI A., EL OUALI A., LAHJOUI A. 2020. Assessment of the risk of soil erosion using RUSLE method and SWAT model at the M'dez Watershed, Middle Atlas, Morocco. In: E3S Web of Conferences. EDP Sciences. Vol. 150, 03014. DOI 10.1051/e3sconf/202015003014.
- BRYAN R.B. 2020. Soil erodibility and processes of water erosion on hillslope. *Geomorphology*. Vol. 32 (3–4) p. 385–415. DOI 10.1016/S0169-555X(99)00105-1.
- CHUENCHUM P., XU M., TANG W. 2020. Estimation of soil erosion and sediment yield in the Lancang–Mekong River using the modified revised universal soil loss equation and GIS techniques. *Water*. Vol. 12(1), 135. DOI 10.3390/w12010135.
- CLARK M.L. 2015. Using GIS and the RUSLE model to create an index of potential soil erosion at the large basin scale and discussing the implications for water planning and land management in Morocco [online]. Austin. University of Texas. [Access 10.12.2020]. Available at: <https://repositories.lib.utexas.edu/handle/2152/35476>
- EL JAZOULI A.E., BARAKAT A., KHELLOUK R., RAIS J., BAGHDADI M.E., 2019. Remote sensing and GIS techniques for prediction of land use land cover change effects on soil erosion in the high basin of the Oum Er Rbia River (Morocco). *Remote Sensing Applications: Society and Environment*. Vol. 13 p. 361–374. DOI 10.1016/j.rsase.2018.12.004.
- FAO 2014. AQUASTAT database [online]. Rome. Food and Agricultural Organization of the United Nations. [Access 10.12.2020]. Available at: <https://www.fao.org/aquastat/statistics/query/index.html>
- Ferreira V.A., Weesies G.A., Yoder D.C., Foster G.R., Renard K.G. 1995. The site and condition specific nature of sensitivity analysis. *Journal of Soil and Water Conservation*. Vol. 50(5) p. 493–497.
- Foster G.R., Toy T.E., Renard K.G. 2003. Comparison of the USLE, RUSLE1.06c, and RUSLE2 for application to highly disturbed lands [online]. In: First Interagency Conference on Research in Watersheds. Washington, DC. US Department of Agriculture, Agricultural Research Service p. 154–160. [Access 20.11.2020]. Available at: <https://citeseerx.ist.psu.edu/viewdoc/download?doi=10.1.1.462.6311&rep=rep1&type=pdf>
- GARCÍA-RUIZ J.M., NADAL-ROMERO E., LANA-RENAULT N., BEGUERÍA S. 2013. Erosion in Mediterranean landscapes: Changes and future challenges. *Geomorphology*. Vol. 198 p. 20–36. DOI 10.1016/j.geomorph.2013.05.023.
- GASHAW T., WORQLUL A.W., DILE Y.T., ADDISU S., BANTIDER A., ZEKEKE G. 2020. Evaluating potential impacts of land management practices



- on soil erosion in the Gilgel Abay watershed, upper Blue Nile basin. *Heliyon*. Vol. 6(8), e04777. DOI 10.1016/j.heliyon.2020.e04777.
- GHOSAL K., BHATTACHARYA S. 2020. A review of RUSLE model. *Journal of the Indian Society of Remote Sensing*. Vol. 48(4) p. 689–707. DOI 10.1007/s12524-019-01097-0.
- GOURFI A., DAOUDI L., DE VENTE J. 2020. A new simple approach to assess sediment yield at a large scale with high landscape diversity: an example of Morocco. *Journal of African Earth Sciences*. Vol. 168, 103871. DOI 10.1016/j.jafrearsci.2020.103871.
- HARA F., ACHAB M., EMRAN A., MAHE G. 2020. Study of soil erosion risks using RUSLE Model and remote sensing: Case of the Bouregreg watershed (Morocco). *Proceedings of the International Association of Hydrological Sciences*. Vol. 383 p. 159–162. DOI 10.5194/piahs-383-159-2020.
- IBRAHIMI S., DAMNATI B., RADAKOVITCH O., HASSOUNI K., SIMON B. 2005. Using conversion models to estimate soil erosion and deposition rates, from the <sup>137</sup>Cs measurements in cultivated soils (north Morocco). *Revista de la Sociedad Geologica de Espana*. Vol. 18 (3–4) p. 217–224.
- KESSTRA S.D., BOUMA J., WALLINGA J., TITTONELL P., SMITH P., CERDÀ A., ..., FRESCO L.O. 2016. The significance of soils and soil science towards realization of the United Nations Sustainable Development Goals. *Soil*. Vol. 2(2) p. 111–128. DOI 10.5194/soil-2-111-2016.
- KIJOWSKA-STRUGALA M., BUCALA-HRABIA A., DEMCZUK P. 2018. Long-term impact of land use changes on soil erosion in an agricultural catchment (in the Western Polish Carpathians). *Land Degradation & Development*. Vol. 29(6) p. 1871–1884. DOI 10.1002/ldr.2936.
- KINNELL P.I.A. 2010. Event soil loss, runoff and the Universal Soil Loss Equation family of models: A review. *Journal of Hydrology*. Vol. 385(1–4) p. 384–397. DOI 10.1016/j.jhydrol.2010.01.024.
- LAHLAOI H., RHINANE H., HILALI A., LAHSSINI S., KHALILE L. 2015. Potential erosion risk calculation using remote sensing and GIS in Oued El Maleh Watershed, Morocco. *Journal of Geographic Information System*. Vol. 7(2) p. 128–139. DOI 10.4236/jgis.2015.72012.
- LAHLOU A. 1986. Updated study of dams' siltation in Morocco. *Water Science Journal*. No. 6, 337356.
- LAL R. 2019. Accelerated soil erosion as a source of atmospheric CO<sub>2</sub>. *Soil and Tillage Research*. Vol. 188 p. 35–40. DOI 10.1016/j.still.2018.02.001.
- LAOUINA A., MAHE G. 2013. Sustainable Land Management. *Proceedings of the multi-stakeholder meeting on the Bouregreg basin May 28, 2013* [online]. Rabat. Association for Research in Sustainable Land Management. ISBN 978-9954-33-482-9. [Access 20.11.2020]. Available at: <http://www.abhatoo.net.ma/content/download/30362/656090/version/1/file/Gestion+durable+des+terres++Proceedings+de+la+R%C3%A9union+multi-acteurs%2C+sur+le+bassin+du+Bouregreg+28+mai+2013.pdf>
- MANAOUCH M., ZOUAGUI A., FENJIRI I. 2021. A review of soil erosion modeling by RUSLE in Morocco: Achievements and limits. In: *E3S Web of Conferences*. EDP Sciences. Vol. 234, 00067. DOI 10.1051/e3sconf/202123400067.
- MAQSOOM A., ASLAM B., HASSAN U., KAZMI Z.A., SODANGI M., TUFAIL R.F., FAROOQ D. 2020. Geospatial assessment of soil erosion intensity and sediment yield using the revised universal soil loss equation (RUSLE) model. *ISPRS International Journal of Geo-Information*. Vol. 9(6), 356. DOI 10.3390/ijgi9060356.
- MARKHI A., LAFTOUHI N., GRUSSON Y., SOULAIMANI A. 2019. Assessment of potential soil erosion and sediment yield in the semi-arid N'fis basin (High Atlas, Morocco) using the SWAT model. *Acta Geophysica*. Vol. 67. No. 1 p. 263–272. DOI 10.1007/s11600-019-00251-z.
- MEYER L.D. 1965. Simulation of rainfall for soil erosion research. *Transactions of the ASAE*. Vol. 8(1) p. 0063–0065. DOI 10.13031/2013.4042.
- NAPOLI M., CECCHI S., ORLANDINI S., MUGNAI G., ZANCHI C.A. 2016. Simulation of field-measured soil loss in Mediterranean hilly areas (Chianti, Italy) with RUSLE. *Catena*. Vol. 145 p. 246–256. DOI 10.1016/j.catena.2016.06.018.
- OSTOVARI Y., GHORBANI-DASHTAKI S., BAHRAMI H.-A., NADERI M., DEMATTE J.A.M. 2017. Soil loss estimation using RUSLE model, GIS and remote sensing techniques: A case study from the Dembecha Watershed, Northwestern Ethiopia. *Geoderma Regional*. Vol. 11 p. 28–36. DOI 10.1016/j.geodrs.2017.06.003.
- PANAGOS P., BORRELLI P., POESEN J., BALLABIO C., LUGATO E., MEUSBURGER K., MONTANARELLA L., ALEWELL C. 2015. The new assessment of soil loss by water erosion in Europe. *Environmental Science & Policy*. Vol. 54 p. 438–447. DOI 10.1016/j.envsci.2015.08.012.
- RANGO A., ARNOLDUS H.M.J. 1987. Watershed management. Food and Agriculture Organization Technical Papers. Rome. FAO pp. 36.
- RELLINI I., SCOPESE C., OLIVARI S., FIRPO M., MAERKER M. 2019. Assessment of soil erosion risk in a typical Mediterranean environment using a high resolution RUSLE approach (Portofino promontory, NW-Italy). *Journal of Maps*. Vol. 15(2) p. 356–362. DOI 10.1080/17445647.2019.1599452.
- SCHILLING J., FREIER K.P., HERTIG E., SCHEFFRAN J. 2012. Climate change, vulnerability and adaptation in North Africa with focus on Morocco. *Agriculture, Ecosystems & Environment*. Vol. 156 p. 12–26. DOI 10.1016/j.agee.2012.04.021.
- SCHMIDT S., TRESCH S., MEUSBURGER K. 2019. Modification of the RUSLE slope length and steepness factor (LS-factor) based on rainfall experiments at steep alpine grasslands. *Methods*. Vol. 6 p. 219–229. DOI 10.1016/j.mex.2019.01.004.
- TANYAŞ H., KOLAT Ç., SÜZEN M.L. 2015. A new approach to estimate cover-management factor of RUSLE and validation of RUSLE model in the watershed of Kartalkaya Dam. *Journal of Hydrology*. Vol. 528 p. 584–598. DOI 10.1016/j.jhydrol.2015.06.048.
- THOMAS D.L., EVANS R.O., SHIRMOHAMMADI A., ENGEL B.A. 1998. Agricultural non-point source water quality models: their use and application. In: *Water Resources Engineering'98*. Eds. S.R. Abt, J. Young-Pezeshk, C.C. Watson. Florida, FL, USA ASCE. CSREES, EWRI p. 1818–1823.
- TIAN P., ZHU Z., YUE Q., HE Y., ZHANG Z., HAO F., GUO W., CHEN L., LIU M. 2021. Soil erosion assessment by RUSLE with improved P factor and its validation: Case study on mountainous and hilly areas of Hubei Province, China. *International Soil and Water Conservation Research*. Vol. 9(3) p. 433–444. DOI 10.1016/j.iswcr.2021.04.007.
- VAN DER KNIJFF J.M.F., JONES R.J.A., MONTANARELLA L. 1999. Soil erosion risk assessment in Italy [online]. Brussels, Belgium. European Soil Bureau, European Commission pp. 54. [Access 20.11.2020]. Available at: [https://esdac.jrc.ec.europa.eu/ESDB\\_Archive/serae/GRIMM/italia/eritaly.pdf](https://esdac.jrc.ec.europa.eu/ESDB_Archive/serae/GRIMM/italia/eritaly.pdf)
- VAN REMORTEL R.D., MAICHLE R.W., HICKEY R.J. 2004. Computing the LS factor for the Revised Universal Soil Loss Equation through



- array-based slope processing of digital elevation data using a C++ executable. *Computers & Geosciences*. Vol. 30(9–10) p. 1043–1053. DOI [10.1016/j.cageo.2004.08.001](https://doi.org/10.1016/j.cageo.2004.08.001).
- WISCHMEIER W.H., SMITH D.D. 1965. Predicting rainfall-erosion losses from cropland east of the rocky mountains: Guide for selection of practices for soil and water conservation. *Agriculture Handbook*. No. 282. Agricultural Research Service, U.S. Department of Agriculture pp. 47.
- WISCHMEIER W.H., SMITH D.D. 1978. Predicting rainfall erosion losses: A guide to conservation planning. A guide for conservation planning. *Agriculture Handbook*. No. 537. U.S. Department of Agriculture, Science and Education Administration pp. 58.
- YJJOU M., BOUABID R., HMAIDI A.E., ESSAHLAOU A., ABASSI M.E. 2014. Modeling water erosion via GIS and the universal soil loss equation in the Oum Er-Rbia watershed. *The International Journal of Engineering and Science (IJES)*. Vol. 3(8) p. 83–91.
- ZHANG H., YANG Q., LI R., LIU Q., MOORE D., HE P., RITSEMA C.J., GEISSEN V. 2013. Extension of a GIS procedure for calculating the RUSLE equation LS factor. *Computers & Geosciences*. Vol. 52 p. 177–188. DOI [10.1016/j.cageo.2012.09.027](https://doi.org/10.1016/j.cageo.2012.09.027).